Thermal stability of gas phase magnesium nanoparticles

Krishnan, Gopi; Kooi, Bart; Palasantzas, Georgios; Pivak, Yevheniy; Dam, Bernard

Published in:
Journal of Applied Physics

DOI:
10.1063/1.3305453

Publication date:
2010

Thermal stability of gas phase magnesium nanoparticles

Gopi Krishnan,[1] Bart J. Kooi,[1,a)] George Palasantzas,[1,a)] Yevheniy Pivak,[2] and Bernard Dam[3]
[1]*Department of Applied Physics, Zernike Institute for Advanced Materials, University of Groningen, Nijenborgh 4, 9747 AG Groningen, The Netherlands*
[2]*Faculty of Science, VU University, De Boelelaan, 1081, NL-1081 HV Amsterdam, The Netherlands*
[3]*MECS, DelftChem Tech, Faculty of Applied Science, Delft University of Technology, POB 5045, NL-2600 GA Delft, The Netherlands*

(Received 9 October 2009; accepted 6 January 2010; published online 3 March 2010)

In this work we present a unique transmission electron microscopy study of the thermal stability of gas phase synthesized Mg nanoparticles, which have attracted strong interest as high capacity hydrogen storage materials. Indeed, Mg nanoparticles with a MgO shell (~3 nm thick) annealed at 300 °C show evaporation, void formation, and void growth in the Mg core both in vacuum and under a high pressure gas environment. This is mainly due to the outward diffusion and evaporation of Mg with the simultaneously inward diffusion of vacancies leading to void growth (Kirkendall effect). The rate of Mg evaporation and void formation depends on the annealing conditions. In vacuum, and at $T=300$ °C, the complete evaporation of the Mg core takes place (within a few hours) for sizes ~15–20 nm. Void formation and growth has been observed for particles with sizes ~20–50 nm, while stable Mg nanoparticles were observed for sizes >50 nm. Furthermore, even at relative low temperature annealing (as low as 60 °C), void formation and growth occurs in 15–20 nm sized Mg nanoparticles, indicating that voiding will be even more dominant for nanoparticles smaller than 10 nm. Our findings confirm that Mg evaporation and void formation in nanoparticles with sizes less than 50 nm present formidable barriers for their applicability in hydrogen storage, but also could inspire future research directions to overcome these obstacles. © *2010 American Institute of Physics*. [doi:10.1063/1.3305453]

I. INTRODUCTION

Magnesium (Mg) is a light, abundant, and a relatively cheap metal which is attractive for hydrogen storage due to a reversible gravimetrical capacity of 7.6 wt % hydrogen.[1] However, the key features of a successful hydrogen storage material are not only a high hydrogen content, but also favorable thermodynamics and kinetics for hydrogen absorption-desorption cycles.[2,3] Many studies have focused on the modification of the hydrogen kinetics and thermodynamic properties by ball milling Mg with catalyst and alloying elements.[4–7] Although the kinetics could be improved, the thermodynamics was hardly affected and the significant thermal stability of MgH_2 still remains the main obstacle for application of Mg(-alloys) in hydrogen storage.

Metallic nanoparticles are of particular interest because they often show size dependent properties different from bulk matter.[8] Theory calculations predict that a particle size below 2 nm decreases the thermal stability of MgH_2, which will improve the desorption temperature for hydrogen storage.[9,10] According to calculations, the heat of formation increases from 66.9 to 79.5 kJ/mol when the particle size varies from 0.6 to 2 nm and approaches the bulk value (~83.7 kJ/mol) beyond 2 nm.[9] Therefore, much effort has been devoted to the preparation of Mg nanoparticles with sizes below 5 nm by various routes, e.g., electrochemical reduction,[11] solvated metal atom dispersion,[12] carbon supported melt infiltration,[13] and a sonoelectrochemical method.[14] Indeed, it has been reported that the desorption temperature T_d can be decreased to 85 and 115 °C compared to $T_d>350$ °C for bulk Mg.[11,12] Nanoconfinement of MgH_2 nanoparticles incorporated in carbon aerogel scaffold prohibits nanoparticles to coarsen and leads to increased number of hydrogenation/dehydrogenation cycles and with faster dehydrogenation kinetics compared to the ball milled nanostructured materials.[15,16]

However, so far, insufficient attention has been paid to the thermal stability of Mg nanoparticles. Moreover, knowledge and understanding of the structural evolution of Mg nanoparticles during hydrogenation is lacking. Such studies are crucial for hydrogen storage technology and applications based on Mg nanoparticles. Therefore, in this paper we report the effect of thermal annealing (within various conditions) on Mg nanoparticles (as prepared by gas phase synthesis) and discuss their applicability to hydrogen storage.

II. EXPERIMENTAL

The Mg nanoparticles were produced by an NC200U nanoparticle source from Oxford Applied Research.[17] The sample chamber was evacuated to a base pressure of ~1×10^{-8} mbar with a partial oxygen pressure of ~10^{-9} mbar. Supersaturated metal vapor is produced by high pressure magnetron sputtering of a Mg target (99.95% purity obtained from Alpha Aesar) in an inert krypton atmosphere (pressure of ~0.25 mbar). The nanoparticles formed in the aggregation volume are removed fast by the use of helium as a drift

[a)]Authors to whom correspondence should be addressed. Electronic addresses: g.palasantzas@rug.nl and b.j.kooi@rug.nl.

gas. The nanoparticles were deposited on 25 nm thick silicon-nitride membranes, which were used for high resolution transmission electron microscopy (HRTEM) imaging and heating analysis in a JEOL 2010F TEM.[18] *In situ* TEM annealing experiments were performed using a Gatan heating holder, where the temperature is accurately controlled with a Gatan model 901 SmartSet Hot Stage Controller. It employs a proportional-integral-derivative (PID) controller which allows accurate control of the temperature within ± 0.5 °C. A desired final temperature can be reached with a fast ramp rate without overshoot.

III. RESULTS AND DISCUSSION

A. HRTEM analysis of hydrogenated Mg nanoparticles

Figure 1 shows an example of Mg nanoparticles after hydrogenation for 40 h at 280 °C in 10 bar H_2. The formation of MgH_2 hydrides is confirmed by Fourier transform analysis of HRTEM images as shown in Fig. 1. The measured interplanar distance in two orthogonal directions in Fig. 1(a) is $d=0.328\pm0.10$ nm and matches with the interplanar distance $d_{110}=0.319$ nm given in PCPDFWIN (No. 120697). This confirms that the magnesium hydride has the α-rutile MgH_2 phase, where it is viewed along the [001] axis such that the orthogonal (110) and $(1\bar{1}0)$ planes are resolved in the image. In addition to this, we imaged several times (see Appendix) the (101) planes of the α-MgH_2 phase with an interplanar distance $d=0.259\pm0.07$ nm which matches with the PCPDFWIN (No. 120697) value of $d_{101}=0.251$ nm. The analysis of Fig. 1(b) indicates the presence of Mg hydrides with the γ-MgH_2 phase, which has an orthorhombic structure. The measured interplanar distance $d=0.281\pm0.04$ nm matches with $d_{111}=0.284$ nm of the PCPDFWIN file No. 351184. Moreover, the MgH_2 also shows the (020) reflection of the γ phase with an interplanar distance $d=0.274\pm0.03$ nm, matching the $d_{020}=0.272$ nm of the PCPDFWIN file (No. 351184) (see Appendix). Therefore, our results confirm that besides the alpha phase there is also the γ-MgH_2 hydride phase.

Notably, the high temperature (in the range from 250 to 900 °C) and high pressure (10^4–10^5 bar) treatment of the α-MgH_2 phase was discussed in Ref. 19, where a partial transformation of α-MgH_2–γ-MgH_2 takes place in bulk Mg. In contrast we observed the presence of the γ-MgH_2 phase along with the α-MgH_2 in most of the Mg nanoparticle after hydrogenation at 280 °C for 40 h and at 10 bar H_2 pressure. The presence of γ-MgH_2 phase confirms that Mg nanoparticles when hydrogenated, even at the relatively low pressure of 10 bar, undergo a partial transformation of α-MgH_2–γ-MgH_2 phase, while bulk Mg shows a partial transformation of the α-MgH_2 phase only at high pressure (more than three orders of magnitude higher than that of the nanoparticles).

As-deposited Mg nanoparticles show a core/shell structure with a pure Mg core and a MgO shell of (~3 nm thick).[18] Comparison of Mg nanoparticles before and after hydrogenation, Figs. 1(c) and 1(d), shows that an additional amorphous shell has formed around the crystalline MgO, which surrounds a predominantly hollow particle core. Dur-

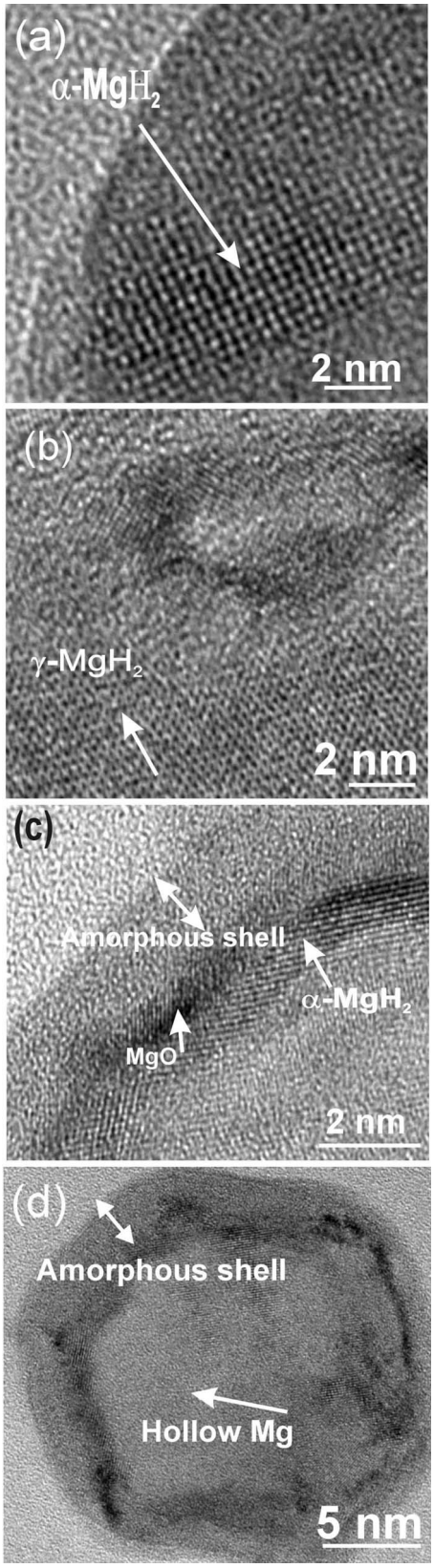

FIG. 1. HRTEM images of Mg nanoparticles after hydrogenation at 280 °C in 10 bar H_2 pressure. (a) α-MgH_2 phase (tetragonal structure) at the periphery of the Mg nanoparticle. (b) γ-MgH_2 phase (orthorhombic structure) as formed in the Mg nanoparticle. (c) Thin α-MgH_2 shell (tetragonal structure) as developed in the vicinity of the intersections of the Mg$\{10\bar{1}0\}$ facets. (d) Hexagonally shaped nanoparticle, where the Mg core has become to large extent hollow, and where an amorphous shell, surrounding the crystalline MgO, has been formed during hydrogenation.

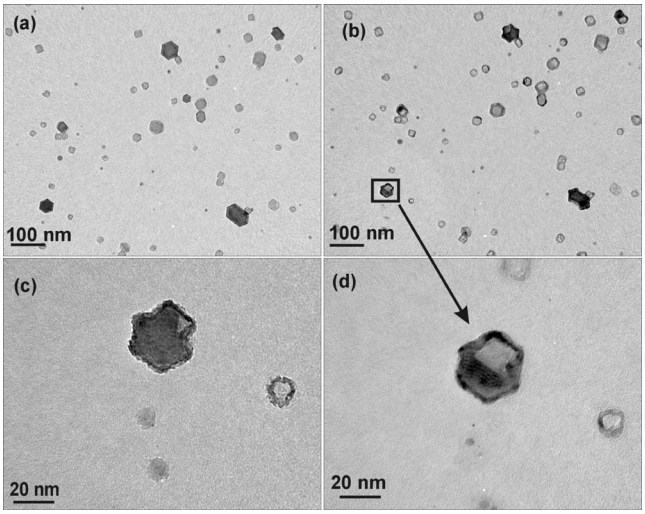

FIG. 2. Bright field images showing the effect of *in situ* TEM (vacuum) annealing at 300 °C on Mg nanoparticles with sizes in the range 10–50 nm. (a) Mg nanoparticles before annealing without voids, (b) the same set of nanoparticles after 5 h of annealing at 300 °C within the TEM; particles with sizes in the range 15–20 nm have formed a completely hollow core (only the MgO shell remains), particles with sizes in the range 20–50 nm show void formation and growth. (c) Mg nanoparticle with a size of 30 nm shows void formation after 1 h of annealing at 300 °C, (d) the same particle after 5 h of annealing showing void growth.

ing hydrogenation of Mg nanoparticles, outward diffusion of Mg takes place accompanied with a simultaneous inward diffusion of vacancies leading to a hollow particle core. After hydrogenation we observe a large void in each Mg nanoparticles, and only a relative thin hydride shell surrounded by a MgO shell remains. The hydride phase preferably forms in the vicinity of the original Mg$\{10\bar{1}0\}$ facet intersections.

An additional important aspect of the hydrogenation experiment leading to the results shown in Fig. 1 is that void formation within the Mg core started earlier than the hydride formation, since annealing is carried out prior to hydrogen introduction therefore only a relatively thin hydride shell developed. This will generally hold for laboratory H_2 dose experiments, where due to the danger of H_2 reacting with O_2 during heating in a closed vessel, first heating is carried out in vacuum and only then H_2 gas is introduced. In our case, the sample was kept for ~1.5 h at 280 °C in vacuum and subsequently H_2 gas was introduced at a pressure of 10 bar. In this respect, it is important to understand what effect vacuum annealing has on Mg nanoparticles, especially at a temperature of 300 °C (or higher) where H_2 absorption and desorption typically takes place.[20,21]

B. Annealing of Mg nanoparticles in vacuum

Figure 2 shows the effect of *in situ* TEM annealing at 300 °C ($\sim 5\times10^{-7}$ mbar) for nanoparticles ranging in size from 10 to 50 nm. It is observed that the Mg nanoparticles with sizes of 15–20 nm suffer from the formation of a completely hollow core, where only the MgO shell remains, even within 2 h of heating at 300 °C. The nanoparticles, which have already a void directly upon deposition (due to oxidation and the associated Kirkendall effect[18]), form a hollow core during 1 h of annealing, while the others without initial

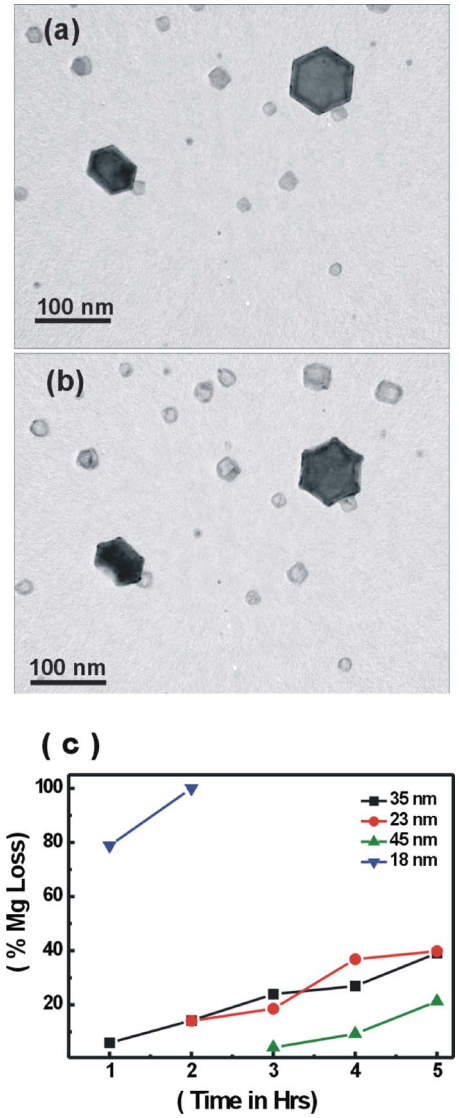

FIG. 3. (Color online) (a) Mg nanoparticles prior to annealing. (b) Mg nanoparticles above 50 nm do not form an observable void within 5 h (*in situ* TEM) vacuum annealing at 300 °C. (c) Areal percentage of Mg loss as a function of annealing time up to a total time of 5 h annealing at 300 °C in vacuum showing an increase in Mg loss with decreasing particle size.

void form a void within 1 h annealing, and a completely hol1ow core within 2 h of annealing. Furthermore, Mg nanoparticles with sizes in the range 20–50 nm form a void and show void growth within 5 h of annealing at 300 °C without, however, forming a completely hollow core. Figures 3(a) and 3(b) show Mg nanoparticles larger than 50 nm, where no longer a void forms within 5 h of annealing.

The void formation process can be attributed to the so-called Kirkendall effect. This effect generally occurs with processes such as oxidation, nitridation, and sulfidation. Basically it refers to a faster outward diffusion of cations compared to an inward diffusion of anions, where the amount of outward material flow is compensated with an inward flow of vacancies, which can finally cluster to form a void. In our case we observe a similar Kirkendall effect but it is now predominantly associated with evaporation. Oxidation in general has a negligible effect since we do not observe oxide shell (crystalline MgO) thickening. In fact, the vapor pres-

sure (P_s) of nanoparticles with a highly curved surface is much higher than that for a flat surface (P_{s0}) following the Kelvin Eq. (1),[22,23]

$$\frac{P_s}{P_{s0}} = \exp\left(\frac{4\gamma M}{\rho_p RTd}\right), \tag{1}$$

where γ is the surface energy, M is the molecular weight, ρ_p is the density of the particle, R is the gas constant, T is the temperature, and d is the particle size. The latter shows that the driving force for evaporation is much higher in case of nanoparticles than for bulk Mg.[22,23] The ratio of the vapor pressure of 10–50 nm Mg nanoparticles based on Eq. (1) at 300 °C after inserting realistic values for Mg (bulk; using γ=0.63 J/m^2 at 300 °C) shows that the driving force for Mg evaporation for 10 nm nanoparticles is more than 13 orders of magnitude higher than a nanoparticle with size of 50 nm. The latter confirms that the smaller Mg nanoparticles will be evaporating much faster than the larger ones, and the driving force to reach the equilibrium vapor pressure (thermodynamic equilibrium with its metallic Mg) triggers the outward diffusion of Mg with simultaneous inward diffusion of vacancies, which cluster to form voids.

Figures 2, 3(a), and 3(b) clearly confirm that there is a thermodynamic effect (small particles influenced more than larger ones) during vacuum annealing leading to hollow-core formation of nanoparticles with sizes 10–80 nm and not only a kinetic effect explaining the Mg evaporation.[23] In addition, as Fig. 3(c) indicates, the areal percentage of Mg loss in different sized nanoparticles shows that with sizes <20 nm the loss is much faster than with sizes larger than 20 nm. From the analysis up to now it can be concluded that the void formation in Mg nanoparticles during vacuum annealing is size dependent and is driven by the outward diffusion of Mg (evaporation associated Kirkendall effect) with simultaneous inward diffusion of vacancies. The size dependence can be readily understood on the basis of the Kelvin equation, leading to an increased driving force for evaporation with decreasing particle size, as already explained above.[22,23]

C. Influence of hydrogenation sequence

To address a pitfall of the hydrogenation experiments that led to the results presented in Sec. III A (cf. Fig. 1), where first annealing in vacuum is performed before H_2 is introduced resulting in void formation before hydride formation. Therefore, we will now present results with the reversed sequence. First we introduced hydrogen gas at a pressure of 5 bar in a closed vessel, which was prepumped to a pressure of 10^{-2} mbar, and only then the samples were annealed at temperature of 300 °C. From Figs. 4(a) and 4(b), showing TEM images acquired after 1 h annealing under these conditions, it becomes evident that voids in Mg nanoparticles with sizes 15–50 nm develop even faster than during annealing in vacuum. In this case, during annealing the Mg vapor probably condensates on the walls instead of creating a vapor pressure and this leads to a high driving force for evaporation (due to the large difference between the actual and the equilibrium vapor pressure).

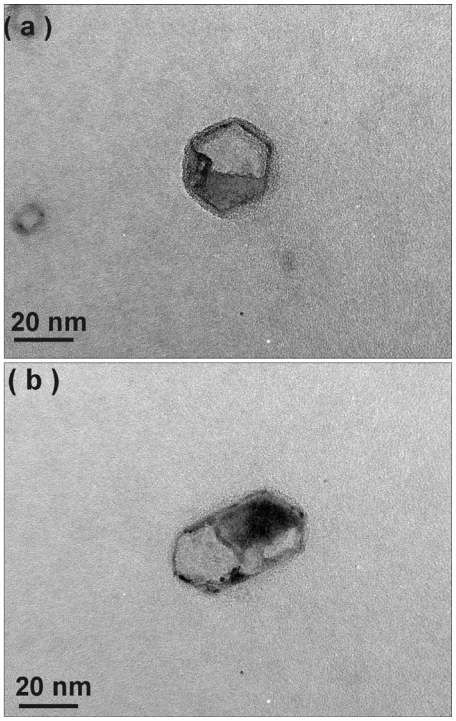

FIG. 4. Void formation and void growth in Mg nanoparticles (sizes 33 and 27 nm) after 1 h of annealing at 300 °C with introduction of 5 bar hydrogen prior to heating.

Moreover, we cannot completely exclude that fact that the introduction of hydrogen prior to heating can increase the defect density in MgO and thereby increasing the diffusivity of Mg. During vacuum annealing the removal of Mg vapor is apparently not so fast and therefore the Mg evaporation is slower. Figure 4 indicates also that rate of formation of MgH_2 is very slow compared to the rate of the Mg evaporation, which makes the void formation and its growth very fast. These results also show that there is a high energy barrier for MgH_2 nucleation and high activation barrier of hydrogen splitting, which finally delays the hydrogenation process. On the other hand evaporation growth is not nucleation controlled and it takes place first. These results and the ones that will be shown directly below clearly indicate that there is a major effect of the surrounding environment on the Mg evaporation rate.

D. Annealing of Mg nanoparticles in argon gas flow

Furthermore, if we consider the practical application of this type of Mg nanoparticles for hydrogen storage in tanks, then it is also important to understand how they would behave during annealing under a flow of gas simulating desorption and absorption of H_2. Annealing of Mg nanoparticles in a flow of argon (at 1 bar pressure) reveals that nanoparticles with sizes in the range 10–50 nm form a hollow core within 2 h. Figure 5(a) shows that after 2 h of annealing a 30 nm Mg nanoparticle forms a completely hollow core, with only the MgO shell remaining, whereas a 45 nm nanoparticle in Fig. 5(b) is only partially hollow. Also in this case the Mg vapor is removed very fast by a flow of argon gas, which

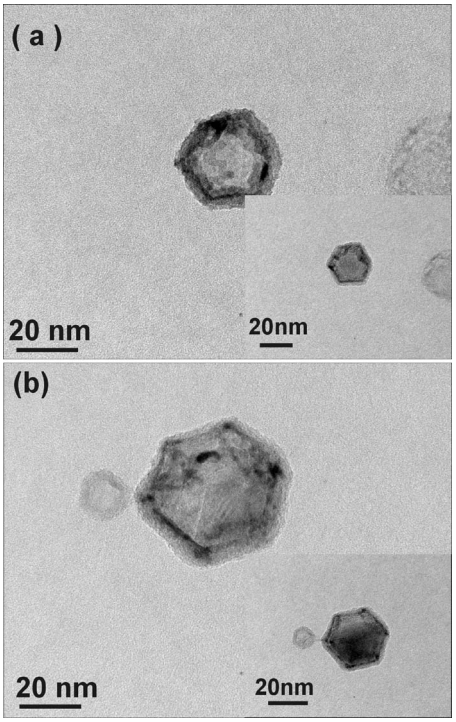

FIG. 5. (a) Mg nanoparticle with a size of 30 nm showing a completely hollow core within 2 h of annealing at 300 °C in an Ar gas flow (the inset shows the same nanoparticle after 1 h annealing). (b) Mg nanoparticle with a size of 45 nm showing an almost hollow core and an amorphous shell around the crystalline MgO after 2 h of annealing in an argon flow at 300 °C (the inset shows the same nanoparticle after 1 h annealing).

leads to a high driving force for evaporation (due to the large difference between the actual and the equilibrium vapor pressure) and thus a high evaporation rate.

E. Annealing of small (<10 nm) Mg nanoparticles

Finally, it remains to be considered what happens during annealing of Mg nanoparticles having sizes below 10 nm. In fact, there has been great interest for Mg nanoparticles with sizes below 5 nm because there are indications that the kinetics and thermodynamics of hydrogen absorption/desorption with respect to that of bulk Mg are improved.[11,12] In recent publications of Mg nanoparticles with size <5 nm produced by various methods, it was shown that H_2 absorption and desorption is possible at relatively low temperatures, ~100 °C, in comparison with the bigger nanoparticles which required about 300 °C.[11,12] Moreover, in Mg-based multilayers, it was shown that the equilibrium pressure is modified by two orders of magnitude, when a thin film is clamped by surrounding Pd layers.[24] We find here that the annealing of Mg nanoparticles (prepared from gas phase synthesis) in vacuum at 60 °C for 24 h leads to voids in the smaller nanoparticles of size ~15–20 nm [Figs. 6(a) and 6(b)]. From our previous experiments, we expect the void formation to be even faster when annealing takes place out of the vacuum.

Therefore, if Mg nanoparticles in the size range 15–20 nm undergo significant voiding at 60 °C, then particles with sizes <5 nm would quickly become completely hollow by heating at 100 °C. As a matter of fact it was impossible for

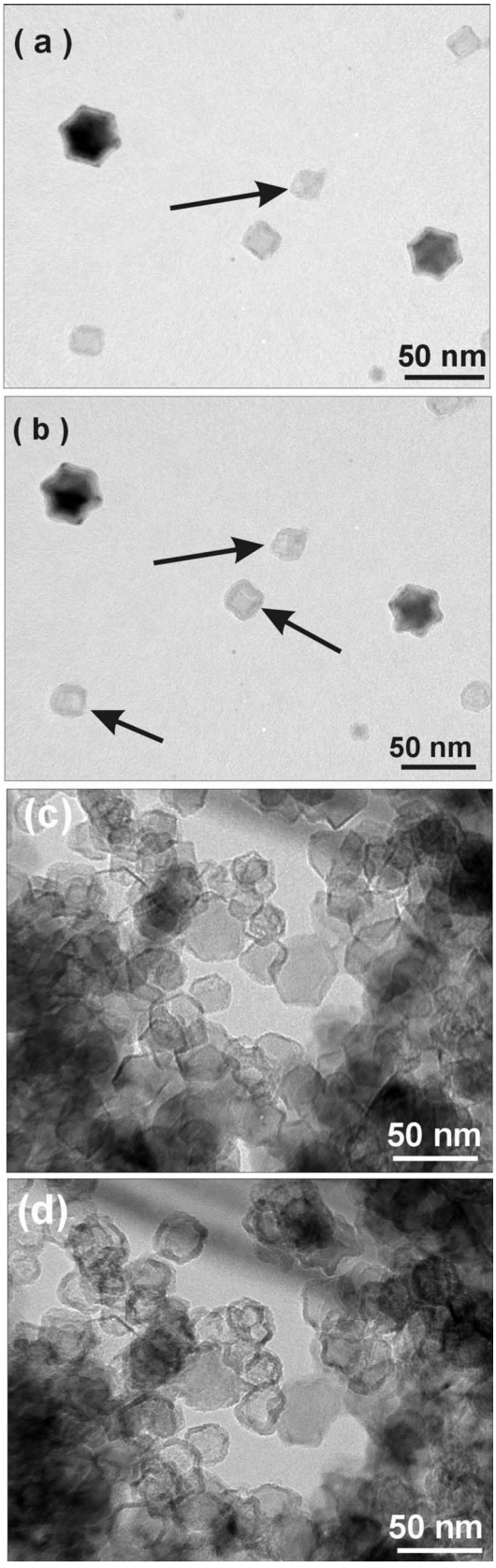

FIG. 6. (a) Mg nanoparticles with sizes in-between 15–35 nm with a void in one of the nanoparticles formed during deposition as the arrow indicates. (b) The same set of Mg nanoparticles after annealing at 60 °C for 24 h showing void formation, and void growth in particles having a size of ~15–20 nm. TEM images of Mg nanoparticle assembled film before (c) and after (d) vacuum annealing for 5 h at 300 °C leading to the same void formation as observed for individual nanoparticles under the same conditions.

us to produce nonhollow Mg nanoparticles with sizes below 10 nm using the gas phase synthesis (due to Kirkendall effect associated with oxidation), which cannot be prevented for gas-phase produced Mg nanoparticles even in a high to ultrahigh vacuum environment. Note that for Mg nanoparticles prepared by other methods in the size range below 5 nm no explicit discussion or consideration is given to the Kirkendall effect associated with oxidation.[11–14]

F. Annealing of nanoparticle assembled films

Having completed our analysis of the annealing behavior of individual Mg nanoparticles at various critical conditions, it is also important to investigate the effect of annealing on Mg nanoparticle assembled film, which is more relevant for H-storage applications. Results of these studies on the Mg nanoparticle assembled films show the same effects as observed for individual nanoparticles in vacuum. The Mg nanoparticle assembled film imaged in Figs. 6(c) and 6(d) shows that after heating for 5 h at 300 °C in vacuum hollow core s are formed in generally all particles. Continuous observation of the Mg nanoparticle films at 1 h intervals at 300 °C for 5 h revealed that nanoparticles with sizes 10–80 nm behave the same way as the individual nanoparticles. Therefore, it is likely that the Mg nanoparticle film will also behave in the same way as it was noticed for individual nanoparticles in all other conditions. Our TEM observations show that there is no coalescence of these nanoparticles up to 5 h of annealing, which is probably explained by the dense MgO shell (3–4 nm thick) around each nanoparticle, which prevents aggregation.

This is similar to the nanoconfinement of MgH_2 nanoparticles incorporated in carbon aerogel scaffold as discussed in Refs. 15 and 16. The MgO shell around the Mg core confines the Mg nanoparticle, which forces it to maintain its nanoscale identity and never leads to coarsening even after annealing for long periods. During annealing the MgO crystalline shell act as a diffusion barrier for the Mg diffusion and subsequent evaporation delaying the formation of the hollow Mg core. Similarly the dehydrogenation of MgH_2 nanoparticle at (T_d) confined in a carbon aerogel scaffold, will also provide an indication of how the Mg evaporation rate varies as compared with the system MgO shell/Mg core.

IV. CONCLUSIONS

Mg nanoparticles with sizes in-between 10–50 nm show the formation of voids and hollow cores, i.e., only the (~3 nm) MgO shell remains after heating at 300 °C for a few hours (in various conditions). Nanoparticles with sizes of 15–20 nm develop a hollow core within 1–2 h of annealing (in vacuum) at 300 °C. Even annealing at a temperature as low as 60 °C for 24 h in vacuum results in void formation and void growth in 15–20 nm in size particles. The above results hold for individual nanoparticles, but also for nanoparticle assembled films. Mg nanoparticles with sizes smaller than 10–15 nm already develop a hollow core when they are produced by an UHV based technique due to oxidation and the associated Kirkendall effect. Therefore, it seems impossible to devise a technique that can produce protected Mg

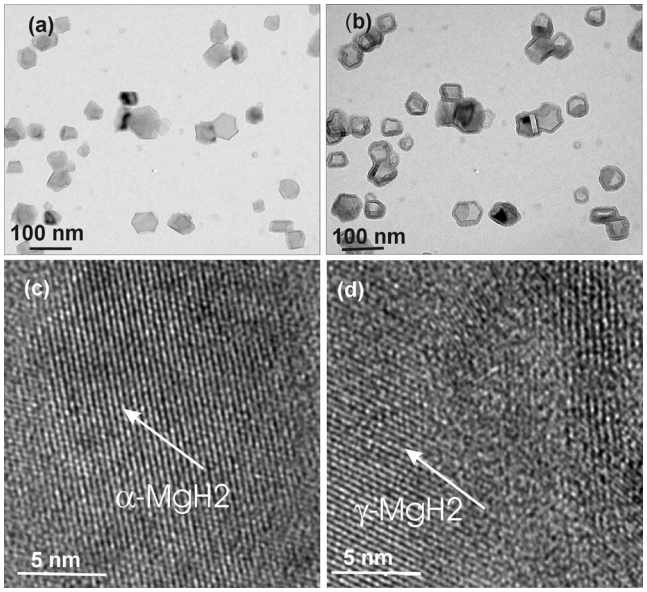

FIG. 7. (a) Mg nanoparticle with sizes in the range 10–80 nm before heating in a TEM. (b) The same set of Mg nanoparticles with the accelerating effect of the electron beam on the Mg evaporation, void formation, and void growth during 40 min continuous observation. (c) HRTEM image of the α-MgH_2 phase where the (101) plane is resolved. (d) HRTEM image of the α-MgH_2 phase where the (020) plane is resolved.

nanoparticles with sizes below 10 nm. Even if they could be produced, the present results prove that these particles are not sufficiently stable, even with a protecting MgO shell during annealing at relatively low temperatures (as low as 60 °C). Moreover, Mg nanoparticles with a size above 50 nm appear sufficiently stable to be used for hydrogen storage, but their size is too big to alter kinetics and thermodynamics drastically from that of bulk Mg. In any case, the present results not only outline the formidable limitations of Mg nanoparticles for application in hydrogen storage but also could inspire future research directions to overcome these obstacles.

ACKNOWLEDGMENTS

We thank The Zernike Institute for Advanced Materials for the financial support. Financial support under the EU project "NessHy" (Novel Efficient Solid Storage for Hydrogen, Contract No. 518271) is gratefully acknowledged. We would also like to acknowledge valuable support of J.Th.M. De Hosson and D. Vainshtein for helping to build the experimental set up for hydrogen storage experiments.

APPENDIX: ELECTRON BEAM EFFECT

The *in situ* heating in the TEM was performed without exposing the sample to the electron beam, so that there is no accelerating effect on the Mg evaporation or void formation due to the electron beam. Figure 7(b) shows the effect of the electron beam irradiation on the Mg nanoparticles when they were continuously observed in the TEM for 40 min. Figure 7(c) shows the HRTEM image of the α-MgH_2 phase, where the (101) plane is resolved with an interplanar distance $d_{101} = 0.259 \pm 0.07$ nm as discussed in the main text of the manuscript. Figure 7(d) shows the γ-MgH_2, where the (020) plane

is resolved with an interplanar distance $d_{020} = 0.274 \pm 0.03$ nm as discussed in the main text of the manuscript. Many times we measured in HRTEM images a *d*-spacing with a value of about 3.3 Å, which is in between the d_{110} of the alpha and the d_{110} of the gamma phase. Therefore, this *d*-spacing did, unfortunately, not allow the identification of either the α-MgH_2 or the γ-MgH_2 phase.

[1] L. Schlapbach and A. Züttel, Nature (London) **414**, 353 (2001).
[2] W. Grochala and P. P. Edwards, Chem. Rev. (Washington, D.C.) **104**, 1283 (2004).
[3] W. Li, C. Li, C. Zhou, H. Ma, and J. Chen, Angew. Chem., Int. Ed. **45**, 6009 (2006).
[4] Z. Dehouche, J. Goyette, T. K. Bose, J. Huot, and R. Schulz, Nano Lett. **1**, 175 (2001).
[5] O. Friedrichs, F. Aguey-Zinsou, J. R. Ares Fernandez, J. C. Sanchez-Lopez, A. Justo, T. Klassen, R. Bormann, and A. Fernandez, Acta Mater. **54**, 105 (2006).
[6] A. Zaluska, L. Zaluski, and J. O. Störm-Olsen, Appl. Phys. A: Mater. Sci. Process. **72**, 157 (2001).
[7] P. Tessier and E. Akiba, J. Alloys Compd. **293–295**, 400 (1999).
[8] C. N. R. Rao, A. Müller, and A. K. Cheetham, *The Chemistry of Nanomaterials: Synthesis, Properties and Applications* (Wiley-VCH, Weinheim, Germany, 2004).
[9] S. Cheung, W. Q. Deng, A. C. T. Van Duin, and W. A. Goddard, J. Phys. Chem. A **109**, 851 (2005).
[10] R. W. P. Wagemans, J. H. van Lenthe, P. E. de Jongh, A. J. van Dillen, and K. P. De Jong, J. Am. Chem. Soc. **127**, 16675 (2005).
[11] K.-F. Aguey-Zinsou and J.-R. Ares-Fernandez, Chem. Mater. **20**, 376 (2008).
[12] S. B. Kalidindi and B. R. Jagirdar, Inorg. Chem. **48**, 4524 (2009).
[13] P. E. De Jongh, R. W. P. Wagemans, T. M. Eggenhuisen, B. S. Dauvillier, P. B. Radstake, J. D. Meeldijk, J. W. Geus, and K. P. de Jong, Chem. Mater. **19**, 6052 (2007).
[14] I. Haas and A. Gedanken, Chem. Commun. (Cambridge) **2008**, 1795.
[15] S. Zhang, A. F. Gross, S. L. Van Atta, M. Lopez, P. Liu, C. C. Ahn, J. J. Vajo, and C. M. Jensen, Nanotechnology **20**, 204027 (2009).
[16] T. K. Nielsen, K. Manickam, M. Hirscher, F. Besenbacher, and T. R. Jensen, ACS Nano **3**, 3521 (2009).
[17] http://www.oaresearch.co.uk.
[18] B. J. Kooi, G. Palasantzas, and J. T. H. M. de Hosson, Appl. Phys. Lett. **89**, 161914 (2006).
[19] L. Zhang, Y. Wang, T. Cui, Y. Li, Y. Li, Z. He, Y. Ma, and G. Zou, Phys. Rev. B **75**, 144109 (2007).
[20] L. Pasquini, E. Callini, E. Piscopiello, A. Montone, M. Vittori Antisari, and E. Bonetti, Appl. Phys. Lett. **94**, 041918 (2009).
[21] O. Friedrichs, L. Kolodziejczyk, J. C. Sanchez-Lopez, A. Fernandez, L. Lyubenova, D. Zander, U. Koster, K. F. Aguey-Zinsou, T. Klassen, and R. Bormann, J. Alloys Compd. **463**, 539 (2008).
[22] W. Thomson, Philos. Mag. **42**, 448 (1871).
[23] K. K. Nanda, F. E. Kruis, and H. Fissan, Phys. Rev. Lett. **89**, 256103 (2002).
[24] A. Baldi, M. Gonzalez-Silveira, V. Palmisano, B. Dam, and R. Griessen, Phys. Rev. Lett. **102**, 226102 (2009).